

# Simplifying Telerobotics

*Wearability and Teleimpedance Improve Human–Robot Interactions in Teleoperation*



MAN—©ISTOCKPHOTO.COM/VCHAN, BLACK GLOVE—©ISTOCKPHOTO.COM/LONGER

---

By Simone Fani, Simone Ciotti, Manuel G. Catalano, Giorgio Grioli, Alessandro Tognetti, Gaetano Valenza, Arash Ajoudani, and Matteo Bianchi

In recent years, wearability has become a new fundamental requirement for an effective and lightweight design of human–robot interfaces. Among the different application fields, robotic teleoperation represents the ideal scenario that can largely benefit from wearability to reduce constraints to the human workspace (acting as a master) and enable an intuitive and simplified information exchange within the teleoperator system. This effective simplification is

particularly important if we consider the interaction with synergy-inspired robotic devices, i.e., those that are endowed with a reduced number of control inputs and sensors, with the goal of simplifying control and communication among humans and robots. In this article, we present an integrated approach for augmented teleoperation where wearable hand/arm pose undersensing and haptic feedback devices are combined with teleimpedance (TI) techniques for the simplified yet effective position and stiffness control of a synergy-inspired robotic manipulator in real time. The slave robot consists of a KUKA lightweight robotic arm equipped

with the Pisa/IIT SoftHand, both controlled in impedance to perform a drilling task—an illustrative example of a dynamic task with environmental constraints. The experimental results from ten healthy subjects suggest that the proposed integrated interface enables the master to appropriately regulate the stiffness and pose of the robotic hand-arm system through the perception of interaction forces and vision, contributing to successful and intuitive executions of the remote task. The achieved performance is presented in comparison to the reduced versions of the integrated system, in which either TI control or wearable feedback is excluded.

## The Motivation for Improving Human–Robotic Interaction

Bilateral robotic teleoperation, called *telerobotics* (distance robotics), with force feedback sent to the user, represents a well-studied problem in literature. The ideal goal is to enable the user to not only interact with the remote environment but also perceive it as if it were being touched directly. At the same time, due to the closed-loop operation of the system, the stability of the master–slave control loop should also be ensured. In the literature, the tradeoff between transparency and stability has been elucidated by several important studies [1], [2]. For example, while force feedback is essential to increase the realism and effectiveness of the interaction in teleoperation tasks, avoiding instabilities due to the presence of latencies in the communication channel is challenging.

The different approaches for stable teleoperation include passivity-based approaches (see, e.g., [3]) and the virtual environment-based approach (see, e.g., [4]). Passivity-based approaches analyze the system's energy flow and imply a sufficient but unnecessary (and also overly conservative) condition for stability. The virtual environment-based approach generates a geometric and dynamic model of the remote physical environment. Other techniques rely on the substitution of grounded kinesthetic force feedback [5] with other forms of feedback, such as visual/auditory or purely tactile [6], or scaling down the kinesthetic feedback to satisfy passivity at the cost of reducing transparency [7]. Visual–haptic feedback can also be combined with a virtual-based approach, as in [8]. In our recent work, we proposed an alternative approach to ensure the stability of teleoperation, TI, which consists of measuring and replicating the master's limb endpoint impedance on the slave robot in real time [9]. Such a direct mapping enables the exploitation of very useful characteristics of the human musculoskeletal system, e.g., energy efficiency, resilience, and safety, that are typical of human behavior and are specifically targeted by the development of soft robots [10]. Nevertheless, effective regulation of the interaction parameters in TI control requires a priori knowledge about the task or a good perception of the environment by the master. Although the integration of grounded force feedback into TI control would be a feasible option, this kind of feedback commonly imposes additional constraints to the human limb and severely limits its overall workspace.

To overcome such limitations and, hence, enhance the transparency and intuitiveness of the human–robot interaction (HRI), wearable systems for haptic rendering and sensing have gained increasing attention in recent years [11]. Wearable haptic systems are mainly thought to deliver tactile cues rather than kinesthetic information, thus ensuring a good tradeoff between stability and transparency. These systems can indeed be comfortably worn by humans, carried around, and integrated into their everyday lives, with ideal applications related (but not limited) to assistive technologies, virtual reality, and telemanipulation of remote robotic systems [12].

TI and wearable haptics/sensing can play a crucial role in telerobotics, especially considering the overall simplification introduced by the concept of synergies, with a special focus on hands. Synergies can be regarded as the main covariation schemes in human hand joints, defining principal patterns of actuation and the sensing of human hands that reduce the burden for control of the human sensory-motor apparatus (see, e.g., [13]). The synergy idea has thus found a fertile field of application in robotics, inspiring the design, control, and sensing of artificial systems with a reduced number of actuators, control inputs, and sensors (see, e.g., [14] for a review on this topic).

Toward the establishment of a teleoperation system that subsumes the advantages of wearable devices and remote impedance control, thereby targeting underactuated synergy-inspired robotic systems, this article integrates our recent results in wearable hand-pose undersensing and haptic feedback for the TI control of a robotic hand-arm system (see Figure 1). The robotic system consists of a lightweight KUKA arm equipped with the Pisa/IIT SoftHand, an anthropomorphic robot hand endowed with 19 degrees of freedom (DoFs) actuated with only one motor, which ensures that the free-hand movement is in accordance with the first human grasping synergy, i.e., the most common pattern of actuation observed in human grasping [13]. SoftHand is also robust yet adaptable and can deform with the external environment to multiply its grasping capabilities [15].

The force feedback on the grasping force exerted by the telecontrolled robotic hand is delivered through a wearable device on the operator's arm [16]. At the same time, to increase the naturalness of the HRI, we track the human limb kinematics and the stiffness profiles through lightweight sensory systems that do not reduce the natural workspace of the master's limb. Furthermore, to enable a more ecological hand pose reconstruction (HPR), i.e., to provide natural inputs for the remote control of the artificial hand, a wearable undersensed solution is exploited. To allow a natural interaction, it is particularly important to avoid cumbersome solutions and, hence, to limit the number of sensors. The HPR is provided for all the joints used for the kinematic hand description but, through a suitable projection technique, only the contribution along the first grasping synergy implemented on the Pisa/IIT SoftHand is considered to command the position of the artificial manipulator in a more reliable manner.

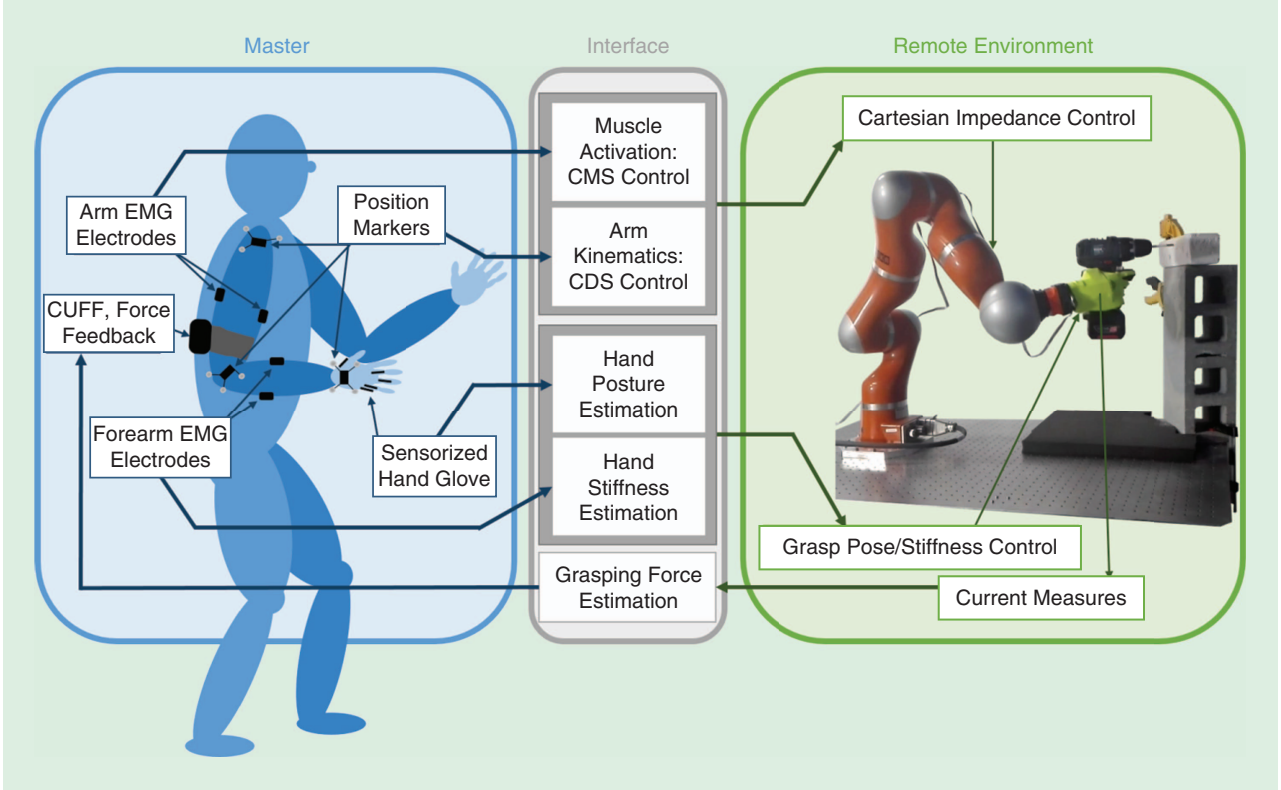


**Figure 1.** The integrated system and experimental setup. CDS: configuration-dependent stiffness; CMS: common-mode stiffness; CUFF: clenching upper-limb force feedback; EMG: electromyography.

Both the robotic hand and arm are controlled in torque. In KUKA, the torque control is computed through torque sensing and actuation [17]. In the Pisa/IIT SoftHand, the torque control is computed through current sensing and control on a custom control board. The tracking of the human hand movements in the direction of the first kinematic hand synergy is achieved through an optimally designed undersensed glove [18] and mapped to the robotic hand in real time. Synchronously, a unidimensional index associates the cocontraction of the human grasp, estimated from one antagonistic pair of forearm muscles [17] to the SoftHand stiffness parameter. An interaction torque observer estimates the forces between the SoftHand and the object, which is fed back to the master using an upper-arm wearable mechanotactile device [16]. The tracking of the human right arm kinematics and its translational Cartesian stiffness components is achieved by reduced-complexity models that exploit minimum sensory data [17], [19] and replicated by the robotic arm's Cartesian impedance controller in real time (decoupled from, but synchronous to, the control of the SoftHand). The proposed interface enables the master to use arm configurations and muscular activations to regulate the pose and stiffness profiles of the robotic hand/arm system to generate task-required forces relying on the visual information and force feedback.

Figure 2 shows a block diagram of the control scheme employed. The values  $\theta_m$ ,  $\theta_{m1}$ , and  $\theta_{m2}$  represent the SoftHand motor and clenching upper-limb force feedback (CUFF) motors angular positions, respectively, while  $\theta_{ref}$  is the syner-

gistic reference configuration (or  $\sigma$ ) commanded to the SoftHand through the glove-based kinematic reconstruction. Furthermore,  $I_m$  is the current absorbed by the SoftHand motor and measured through current readings;  $I_{lut}$  represents the contribution to the reconstructed free-hand motion current due to the angular position, velocity, and acceleration; and  $K_q$ ,  $K_v$ , and  $K_a$  represent the functions related to the motor angular position, velocity, and acceleration, respectively. The term  $r_I$  is used to compute the reference angular motor position of CUFF motors through the proportional factor  $\beta_{CUFF}$ . See [16] for further details.

Conclusively, the integration proposed here contributes to the successful and intuitive execution of remote tasks. The achieved performance is presented in comparison with reduced versions of the integrated system, where either TI control or wearable feedback is excluded.

The inspiration for our work is a generalized simplification strategy informed by the neuroscientific concept of synergies. This idea is used for the development and control of the SoftHand and for the optimal design of HPR. Furthermore, the concept of synergies, intended in a broad sense, has also driven the implementation of TI and force feedback. In TI, synergies led to a simplification of sensing components and methods, while the implementation of force feedback yields the possibility of rendering the overall force exerted by the SoftHand along its motion pattern, relying on an indirect estimation of the force based on the current absorbed by the hand motor without using any extrinsic sensor.

## The Robotic Hand and Arm System

The Pisa/IIT SoftHand [15] is an anthropomorphic hand designed with 19 DoFs, having four on each of the long fingers and three on the thumb. The fingers are capable of flexion/extension as well as abduction/adduction. For abduction/adduction of the fingers and at the equivalent of the carpometacarpal joint of the thumb, traditional revolute joints were employed. The rest of the joints incorporate rolling contact joints with elastic ligaments, which ensure physiologically correct motions when actuated but easily disengage on impact to allow a safe interaction with humans while preserving the hand. The elastic ligaments also allow deformation while ensuring the hand returns to its original configuration. This design enables the SoftHand to softly interact with the environment and adapt to the items, exploiting the external constraints. A single tendon runs though all joints to simultaneously flex and adduct the fingers upon actuation. The hand is actuated by a single dc motor, which moves the fingers on the path of the first synergy [13], hereinafter referred to as  $S$  described in  $\mathbb{R}^{19}$ , allowing the SoftHand to mold around the desired object (see [15] for further details). More information and computer-aided drawing files of this robotic hand can be freely downloaded from the Natural Machine Motion Initiative ([www.naturalmachinemotioninitiative.com/](http://www.naturalmachinemotioninitiative.com/)).

In this article, we used a myoelectric version of the Pisa/IIT SoftHand. More specifically, by exploiting the concept of synergies that drive concurrent muscle activation, only one pair of antagonistic muscles [two surface electromyography (EMG) channels from the major finger antagonist pair, i.e., the extensor digitorum communis (EDC) and flexor digitorum superficialis (FDS)] was used to drive the stiffness and postural synergy references tracked by the hand controller, as detailed later in this article (see also [17]). The hand is mounted over the wrist of a 7 DoF KUKA LWR IV+ arm. The position and endpoint stiffness are controlled using the techniques detailed in the next section.

## Common-Mode and Configuration-Dependent Stiffness Principles for Real-Time Tracking of the Human Arm Endpoint Impedance

There are several important reasons why humans principally explore the control of arm configurations to perform tasks that require dynamic dexterity. One explanation for such a behavior is the ergonomic efficiency of the postural adjustments in the generation of certain endpoint force manipulability or stiffness profiles in comparison to the muscular (co)activations [20]. Another important factor is the major contribution of the arm pose to effective modifications in the geometry of the endpoint stiffness ellipsoid. The latter can be mathematically described by transformations from the muscle stiffness matrix ( $K_m$ ) to the arm joint stiffness ( $K_J$ ) and consequently to the Cartesian stiffness matrix ( $K_c$ ) by

$$K_c(p, q) = J^{+T}(q) [J_m^T(q) K_m J_m(q)] J^+(q), \quad (1)$$

with  $K_J(p, q) = J_m^T(q) \hat{K}_m(p) J_m(q)$ , and  $p, q$  and  $K_m$  being the muscle activation and joint angle vectors and muscle stiffness matrix, respectively; the effects of gravity and external load are neglected in this equation. The quadratic effect of the arm kinematics through arm  $J(q)$  and muscle  $J_m(q)$  Jacobians on the Cartesian stiffness matrix is evident in this equation.

The tracking of the arm kinematics is achieved through a passive marker motion capture system (Vicon) using the concept of arm tangle, as explained in [19]. Three rigid-body markers can be attached to the hand, elbow, and shoulder segments and used for the tracking of the arm Jacobian. Using the muscle attachment points [21] and the length variations over the joint angles, the muscle Jacobian can be computed online.

The effect of muscle stiffness matrix ( $K_m$ ) in joint and endpoint stiffness variations is commonly described using Hill's activation dynamic equations, which provide a mapping between the muscular activities, usually measured by the

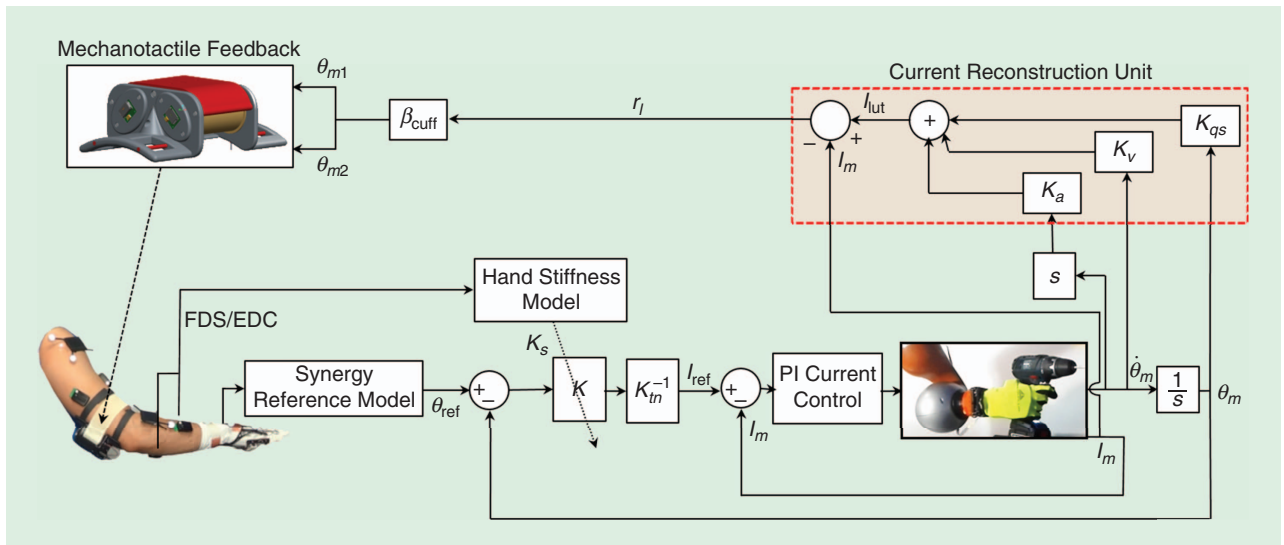


**Figure 2.** A block diagram of the integrated system. EDC: extensor digitorum communis; FDS: flexor digitorum superficialis.

EMGs, and the corresponding muscles' stiffness profiles. This, however, requires the EMG activities of several muscles to be processed and passed through a complex system of equations to account for the muscle stiffness matrix, eventually resulting in a costly (requiring several EMG sensors and amplification) and computationally intensive system. However, the dense literature gives solid evidence for the existence of synergistic relationships between the arm's mono- and biarticular muscle activities, which realize a coordinated stiffening profile across the arm joints [22], [23]. As a result, cocontractions of the arm muscles mostly contribute to the modifications in the volume of the endpoint stiffness ellipsoid rather than to its direction [9]. This strategy is deemed to be exploited by the central nervous system to solve for the motor complexity in an efficient and coordinated manner [24].

On this basis, in our recent work [19], the concepts of common-mode stiffness (CMS) and configuration-dependent stiffness (CDS) were proposed to associate the arm muscular activities and configurations to variations in the volume and major axes orientations of the arm endpoint stiffness ellipsoid, respectively. To design a real-time arm endpoint stiffness model, we presume that 1) a synergistic relationship exists between the arm muscle activities and 2) each muscle activation contributes to the volume of the endpoint stiffness ellipsoid with a different ratio. Accordingly, we propose  $\hat{K}_m = a_{cc}(p) K_s$ , with  $K_s$  as an experimentally identified, time-invariant diagonal matrix that implements the contribution of each muscle to the active variations of the volume of the endpoint stiffness with a certain weight. The scalar and time-varying component,  $a_{cc}(p)$ , which is a function of the muscular activities, is multiplied by the muscle weights to compute the overall contribution of muscle activations to the volume of the endpoint stiffness ellipsoid. Obviously, depending on the choice of muscles that are used for the computation of the active component ( $a_{cc}$ ), the identified scale matrix  $K_s$  would differ. In this study, we process the EMG activity of the biceps brachii (BB) ( $P_B$ ) and triceps brachii (TB) ( $P_T$ ) muscles as the dominant and easily accessible muscles of the arm for surface EMG measurements to calculate  $a_{cc}(p) = c_1 + c_2(P_B + P_T)$ , with  $c_1$  and  $c_2$  being constant coefficients referring to the intrinsic muscle stiffness component. By rearranging the above equations, we obtain

$$K_c(p, q) = J^{+T}(q) [J_m^T(q) a_{cc}(p) K_s J_m(q)] J^+(q). \quad (2)$$

The parameters of such models are subject-specific and must be identified offline. To achieve this, as described in [19], the endpoint stiffness [ $K_c(p, q)$ ] of the human arm was estimated in various arm pose ( $q$ ) and activation levels of the arm muscles ( $P$ ). The stiffness matrix was estimated by applying stochastic position perturbations and measurements of the restoring forces. The estimated stiffness matrices and the measured data [muscle activities ( $P$ ) and arm and muscle Jacobians calculated from  $q$ ] can consequently be used for the identification of the model parameters by minimizing the norm

$$\| J_m^T(q) a_{cc}(p) K_s J_m(q) - J^T(q) K_c(p, q) J(q) \|, \quad (3)$$

with  $J_m \in \mathbb{R}^{8 \times 7}$ ,  $K_s \in \mathbb{R}^{8 \times 8}$ ,  $J \in \mathbb{R}^{3 \times 7}$ , and  $K_c \in \mathbb{R}^{3 \times 3}$  (the only translational components of the stiffness matrix). In this model, we exploit arm muscle length functions of eight dominant muscles acting on the shoulder, elbow, and wrist joint to model the moment arms of the muscles as functions of the corresponding joint angles (see [25].) The eight selected muscles are the anterior and posterior portions of the deltoid, the brachialis, the brachioradialis, the long and short portions of the biceps, and the long and lateral portions of the triceps, which present dominant effects in generation of the torque profiles in the arm joints. Therefore, ten unknown parameters ( $K_s$ ,  $c_1$ , and  $c_2$ ) must be identified that define the minimum number of required trials for the calibration experiments. Based on this number, the total number of trials was divided into the calibration and test trials for the validation of the identified model. The identified matrix  $K_s$  represents the coordinated contributions of the selected muscles to the endpoint stiffness variations. The other two components,  $c_1$  and  $c_2$ , are used for the definition of the scalar value  $a_{cc}$ , which represents the active contribution of muscular activities to the modifications of the volume of the endpoint stiffness matrix [19].

Once the model parameters are identified, (2) can be utilized for the real-time computation of the arm endpoint stiffness profile using EMG signals of one antagonistic pair of muscles and the tracking of the arm triangle (refer to [19] for details). The EMG signals are acquired by the wireless Delsys Trigno system (Delsys Inc.) at 1 kHz. The processing (filtering and normalization to the maximum voluntary contraction) is performed online. The tracking of the arm triangle is achieved by 11 Flex-3 cameras of the Optitrack system (NaturalPoint, Inc.) by attaching three rigid-body markers to the shoulder, elbow, and wrist of the human hand at 100 Hz. Our real-time model enables the master to modify the direction of the endpoint stiffness ellipsoid by changing the arm posture in an intuitive manner while being capable of adjusting its volume by increasing the cocontraction of the dominant arm muscles. As a result, teleoperated tasks that require significant modulation of the endpoint stiffness and force can be effectively and naturally executed.

## A Wearable Approach to the Dynamic Remote Control of a Synergy-Driven Robotic Hand

### A Wearable HPR System: Optimal Design and Undersensing

The position of the Pisa/IIT SoftHand was controlled based on the user's hand posture, which was acquired through a wearable sensing glove. This glove [18] was endowed with five textile goniometers, which can measure five joint angles (see Figure 3). This glove has also been integrated with a tactile sensing glove to provide a tool to retrieve both kinematic and force information from the human hand in grasping

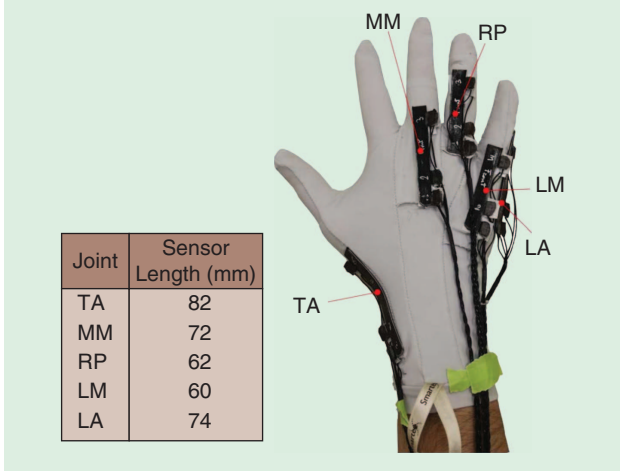


**Figure 3.** A glove with KPF sensors on the joints of interest [18]. LA: little abduction; LM: little metacarpal; MM: middle metacarpal; RP: ring proximal; TA: thumb abduction.

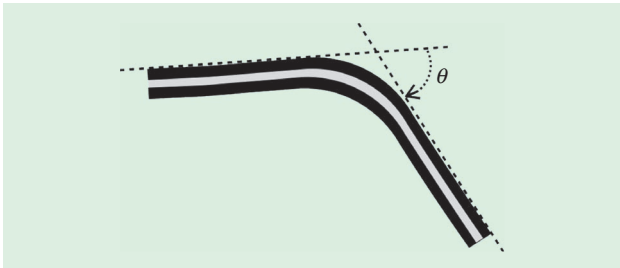


**Figure 4.** A representation of a double-layer textile goniometer [18].

tasks [26]. Textile goniometers consist of two piezoresistive layers connected through an electrically insulating layer. The sensing layers of the textile goniometers were fabricated using knitted piezoresistive fabrics (KPFs). The output of the sensors is the electrical resistance difference computed from the two sensitive layers and is proportional to the flexion angle (see Figure 4) [27]. In Figure 4, the two external stripes represent the piezoresistive layers. The gray line is the electrically insulating layer. The bending angle ( $\theta$ ), represented by the angle between the tangent planes to the goniometer extremities (the black dashed stripe), is proportional to the difference of the resistance ( $\Delta R$ ) of the sensing layers. The distribution of the sensors on the glove was optimal in a Bayesian sense, such that it maximizes the information on the actual hand posture.

The theoretical work that led to the definition of the design guidelines was laid out in [28]: the idea was to exploit hand joint covariation schemes in grasping tasks, or hand synergies [13] as a priori information to complete a hand pose from a limited number of (noisy) measures and, at the same time, to decide how and where to place sensors on the glove, taking into account the knowledge on how humans most frequently use their hands in grasping tasks.

Five KPF goniometers were built and integrated into the glove to fulfill the design requirements (i.e., sensor length) and to measure the following joint angles, according to the

kinematic model in [13], i.e., thumb abduction (TA), middle metacarpal (MM), ring proximal (RP), little abduction (LA), and little metacarpal (LM), respectively. This sensor placement was inspired by the optimal design guidelines in [28]; the measurements KPFs provide were then completed through synergy-based estimation techniques [29] to obtain hand posture reconstruction according to a 19-DoF model. More details on the sensing glove can be found in [18].

#### Kinematic Mapping: From Human Hand to Pisa/IIT SoftHand

Once the hand pose of the user is reconstructed, it is used to control the position of the Pisa/IIT SoftHand, which is built to move without obstacles along the vector of the first human postural synergy  $S$  (in our case,  $S \in \mathbb{R}^{19}$ ), which also represents the reference configuration toward which the real hand position is attracted, and at the same time repelled from, due to the interaction and grasping with the external object, according to the soft synergy model [30]. Since the SoftHand is commanded to move along the first human postural synergy, for this experiment, we need to estimate the value of  $\sigma$ , i.e., the synergy intensity [30], which should be commanded to the SoftHand motor.

Vector  $S$  is implemented in the SoftHand through a careful design of spring elements and pulley trains, resulting in a coordinated closure of all joint angles. To get value  $\sigma$

$$\sigma = S^T x, \quad (4)$$

where vector  $x$  contains the reconstructed human hand joints.

This value needs to be correlated with the SoftHand motor position: to do it, we first get  $\sigma_{\max}$  corresponding to the maximum closure of the human hand and relate it to motor position (in ticks). The other intermediate  $\sigma$  values can be obtained via simple proportion. This reconstruction provides an effective way to command synergy-based robotic hands and can be extended to systems with more degrees of actuation (see e.g., [31]).

#### TI for Intuitive Control of the Robotic Hand

Following the previously described implementation of TI control for the teleoperation of a robotic arm, we explored the translation of this approach to the control of a synergy-driven robotic hand, the Pisa/IIT SoftHand [17]. The reference configuration commanded to the hand is the difference of the two EMG signals from FDS and EDC. These signals were acquired through two surface EMG electrodes by Trigno System. To regulate the stiffness of the hand, we used an EMG-driven P-gain modulation. In other words, the proportional gain of the proportional-integral-derivative controller of the SoftHand motor position control increased with increasing amplitude of the EMG signal with the smallest amplitude, normalized to the signal's highest amplitude. The upper and lower bounds for the proportional gain were estimated through pilot data by selecting the range of values in which the SoftHand moved smoothly until reaching the reference position. Accordingly, the SoftHand movement velocity and

impedance were modified by changing the proportional gain value. More details can be found in [32].

### Wearable Haptic Device for Force Feedback

To convey information about the grasping force produced by the Pisa/IIT SoftHand, we used the CUFF wearable device for the distributed mechanotactile stimulation of normal and tangential skin forces. The device is described in more detail in [16].

The CUFF device can be worn on the user's forearm and is endowed with two independently controlled dc motors. The device design is based on an elastic belt wrapped around the user's limb. For this study, the motors spin in opposite directions to tighten or loosen the band on the arm in accordance with estimated grasp force. In Figure 5, the real prototype and a three-dimensional rendering of the CUFF system are shown, highlighting some details of its mechanical implementation. The CUFF device weighs  $\approx 230$  g, and its overall dimensions are  $12.4 \times 7.0 \times 5.8$  cm.

One possible application of the CUFF device is to enhance the haptic interaction with the environment, in particular, as a haptic feedback device for robotic/prosthetic hands, with the goal of achieving better grasp stability by conveying grip force information [17]. The Pisa/IIT SoftHand was equipped with a custom-made  $\mu$ -controller, which controls the opening/closing level of the hand in position by acting on the current that drives the motor. The complete scheme of the control is represented in Figure 2. The basic idea is to use the hand motor current to provide a rough estimate of the applied force to the external environment. This approach is motivated by the fact that there is a net difference in the motor current, in free motion (with the maximum value  $\approx 800$  mA), or when the robotic hand grasps an external object (with the maximum value  $\approx 1,200$  mA). The CUFF device is then controlled through the residual current  $r_I$ , defined as the difference between the current absorbed by the SoftHand motor and the current reconstructed. The reconstructed current represents the motor current in free hand motion, which will be subtracted from the current sensed by the  $\mu$ -controller. More details can be found in [16].

### Integration and Experimental Tasks

In our experimental setup, we integrated the aforementioned techniques, i.e., TI, sensing, and force feedback. We implemented two control loops. One controlled the sensing glove, the Pisa/IIT SoftHand (both in position and stiffness), and managed the force feedback. The other controlled the KUKA robot through a developed Cartesian impedance controller to replicate the masters' arm endpoint trajectories and stiffness. EMG signals were acquired by a third computer, which broadcast these values over a local wired network. The two control loops, running on two distinct computers, took data of interest directly from the network. These two loops run at a frequency of 100 and 200 Hz, respectively. During the experiments, we asked participants to control the pose and stiffness of the Pisa/IIT SoftHand mounted on KUKA. The arm TI control (described in the "The Robotic Hand and Arm System" sec-

tion) was used to command the position of the robotic arm and regulate the impedance of the system online. The task consisted of grasping a drilling tool and using it to drill a block of autoclaved, aerated concrete. The task was considered successful if the participant could grasp the tool placed on a table, use it to drill the block (to produce a hole with a length of at least 4 cm), and remove the drill from the hole.

Ten right-handed volunteers (eight males and two females, age  $27.4 \pm 2.63$  years) took part in the experimental tests. All participants in these studies gave informed consent to perform the experiments. No subjects reported physical limitations that would affect their ability to perform the task. The participants' average arm length was 29.47 cm from the shoulder to the elbow, with a standard deviation of 2.41 cm, and 24.02 cm from the elbow to the wrist, with a standard deviation of 4.06 cm. The average hand measurements were  $10.21 \pm 0.93$  cm wide (measured from the tip of the thumb to the tip of the little finger in flat hand posture) and  $18.48 \pm 0.79$  cm long (measured from the wrist to the tip of the middle finger). For each subject, fast calibrations for the sensing glove (see the "Common-Mode and Configuration Dependent Stiffness Principles for Real-Time Tracking of the Human Arm Endpoint Impedance" section) and for the TI controllers for the arm and the hand were performed (see the "The Robotic Hand and Arm System" and "Common-Mode and Configuration Dependent Stiffness Principles for Real-Time Tracking of the Human Arm Endpoint Impedance" sections, respectively).

Six experimental conditions were considered: 1) low stiffness (LS), 2) high stiffness (HF), and 3) TI, with and without the use of CUFF force feedback. In the LS condition, the stiffness of the SoftHand was also low; we set the P-gain of the SoftHand controller at 0.005, and the Cartesian stiffness of the KUKA robot was set to 800 N/m and 50 Nm/rad in all translational and rotational directions, respectively. For the

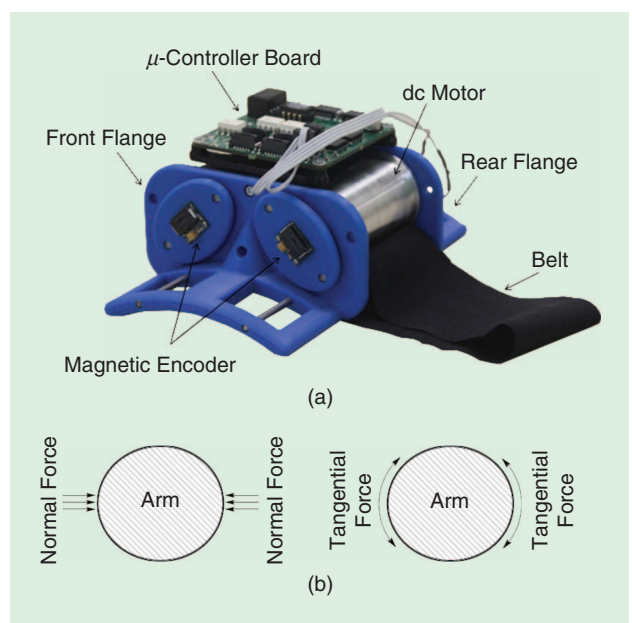


**Figure 5.** A (a) device overview and (b) working modes [16].

HS condition, the P-gain of the SoftHand was set to 0.05, with the KUKA Cartesian stiffness values of 2,000 N/m and 200 Nm/rad in all translational and rotational directions, respectively. These represent the lower and upper bounds, guaranteeing a stable performance. In the TI condition, the P-gain and the robot endpoint stiffness profile were modulated as described in the “Common-Mode and Configuration-Dependent Stiffness Principles for Real-Time Tracking of the Human Arm Endpoint Impedance” section.

At the end of the experiments, we asked subjects to answer the questions using a seven-point bipolar Likert-like scale (see Table 1).

A score of one means completely disagree and seven completely agree.

## Results

As performance evaluation metrics, we considered the success in task accomplishment and modulation of EMG signals and

interaction forces. We will discuss the main experimental outcomes in this section, considering the effect of TI modulation and force feedback. An example of an exemplary trial performed with TI control and force feedback can be found in the accompanying video.

### Success Rate

In Table 2, we report the success rate for the different conditions. TI exhibits the highest success percentage (83.3%), although HS also provides a high success rate (78.3%) with respect to (w.r.t.) LS, which has only 60.0%.

We have performed  $\chi^2$  nonparametric statistical tests considering the relative frequency of succeeding trials between the three different experimental conditions (TI, LS, HS) and for the two factors (CUFF and no CUFF). With the TI condition, the contingency table of observed frequencies is associated with a  $p < 0.085$  ( $\chi^2 = 3$ ,  $df = 1$ ), as calculated considering the Yates correction for the  $\chi^2$  calculation due to

**Table 1. Statements, presented in random order, rated by the subjects using a seven-point Likert scale: 1) Strongly disagree through 7) strongly agree.**

Questions	Median	IQR	CI m. 95%
1) I had the feeling of performing better while receiving force feedback from the cutaneous device.	6	1	(5,6)
2) I had the feeling of performing better while modulating the impedance of the end effector.	6	1	(5,7)
3) I was feeling uncomfortable while using TI with the cutaneous device.	2	0	(1,3)
4) The TI control was intuitive.	6	0	(5,6)
5) I felt hampered by the cutaneous device.	2	0	(1,2)
6) It was easy to move my hand and fingers while wearing the sensing device.	6	0	(4,7)
7) Please rate your impression of how close the robot behaved as an extension of your body.	6	1	(5,7)

IQR: interquartile range; CI m.: confidence interval median.

**Table 2. The success of task accomplishment for the different conditions.**

Subject	TI (%)		LS (%)		HS (%)	
	CUFF	No CUFF	CUFF	No CUFF	CUFF	No CUFF
1)	100.0	100.0	100.0	100.0	66.7	100.0
2)	100.0	66.7	100.0	66.7	100.0	100.0
3)	66.7	33.3	66.7	0.0	66.7	100.0
4)	100.0	100.0	33.3	0.0	33.3	66.7
5)	100.0	66.7	33.3	0.0	100.0	66.7
6)	100.0	66.7	100.0	33.3	100.0	0.0
7)	100.0	100.0	100.0	100.0	100.0	66.7
8)	66.7	0.0	33.3	0.0	66.7	66.7
9)	100.0	100.0	66.7	66.7	100.0	66.7
10)	100.0	100.0	100.0	100.0	100.0	100.0
Total	93.3	73.3	73.3	46.7	83.3	73.3
Total group	83.3		60.0		78.3	

the low value of expected frequencies, meaning that in this experimental condition, the use of the CUFF device tends to increase the chances of success trial rate. Nevertheless, we can only claim this trend because of the formal acceptance of the null-hypothesis considering a statistical significance of 5%. Likely, a higher number of subjects involved in our experimental protocol would allow us to reach a proper statistical significance.

For LS, the contingency table of observed frequencies is associated with a  $p < 0.05$  ( $\chi^2 = 4.44, df = 1$ ), meaning that in this experimental condition, the use of a CUFF device significantly increases the chances of success trial rate. This could be ascribed to the lower force produced by the Soft-Hand, in this case, compared to the other two. In this condition, the information conveyed by the CUFF is essential to make the subject aware that the control he/she is exerting is not sufficient for lifting, carrying, and handling the driller and, hence, can increase the grasping force for a successful task completion.

Considering the HS condition, the contingency table of observed frequencies is associated with a  $p > 0.05$  ( $\chi^2 = 0.884, df = 1$ ), meaning that, in this experimental condition, the use of the CUFF device does not increase the chances of success trial rate. This may be because, in the HS condition, the proportional gain of the SoftHand control is very high, resulting in fast and strong hand movements. These movements generate high grasping forces that can be regulated for difficulty even with the usage of the CUFF device.

Importantly, regardless of the experimental condition, the contingency table of observed frequencies is associated with a  $p < 0.005$  ( $\chi^2 = 8.32, df = 1$ ), demonstrating that in a generic scenario the use of the CUFF device significantly increases the chances of success trial rate.

We then investigated differences in the trial success rate regardless of the use of the CUFF device. In this case, the contingency table of observed frequencies is associated with a  $p < 0.01$  ( $\chi^2 = 9.39, df = 2$ ), meaning that the specific experimental condition does influence the trial success rate. We then performed an  $\chi^2$  post hoc test considering Bonferroni correction of the statistical significance, observing that the TI significantly increases the change of trial success rate with respect to the LS condition ( $p < 0.005$ ,  $\chi^2 = 8.04, df = 1$ ). Other multiple comparisons do not reach the formal statistical significance (as associated with corrected  $p > 0.05$ ), although it is worthwhile noting that the LS versus HS comparison is associated with a corrected  $p < 0.06$  ( $\chi^2 = 4.73, df = 1$ ), meaning that the HS condition tends to increase the change of the trial success rate with respect to the LS condition. The nonstatistical difference between TI and the HS condition could be explained by the fact that, for this task, the HS condition generates very precise movements that lead to a successful trial execution. However, the integrated usage of TI and the CUFF device produces a different modulation of the interaction forces, which are generally lower w.r.t the HS case and suitably adapted to the different phases of the trial. This would result in safer interactions and would be like-

ly to produce reduced fatigue in subjects during longer tasks (see the “Interaction Forces” section).

### Subjective Evaluation

The scores provided by ten participants, which were analyzed through descriptive and inferential statistics, are reported in Table 1, along with the relative data from the statistical analysis. Question 7 refers to the TI condition with CUFF feedback.

Analyzing the data, we can conclude that the cutaneous device and TI increase subjective evaluation of task performance (questions 1 and 2). Participants had the impression that they performed better when TI control and force feedback were provided. Furthermore, the integration of TI and the CUFF device was perceived as comfortable by the subjects, who did not feel hampered by the cutaneous device (questions 3 and 5). The sensing glove for HPR was evaluated as highly wearable, imposing minimal constraint to finger and hand movements (question 6). Regarding the transparency of the system to the user (question 7), the users rated the perception of the robot as an extension of their body when TI and CUFF were used together, providing a very high score.

### EMG Modulation and Hand Interaction Forces

This section reports on the effect of feedback (CUFF device) on the modulation of EMG signals of the EDC and FDS muscles and the consequent grasping forces. Figures 6 and 7 illustrate the typical results of the EMG activities and the corresponding grasping interaction forces of the SoftHand under TI control with and without the haptic feedback, respectively. As observed, the haptic interface enables the user to effectively modulate the EMG activities and the grasp forces to achieve a stable grasp in different phases of the task.

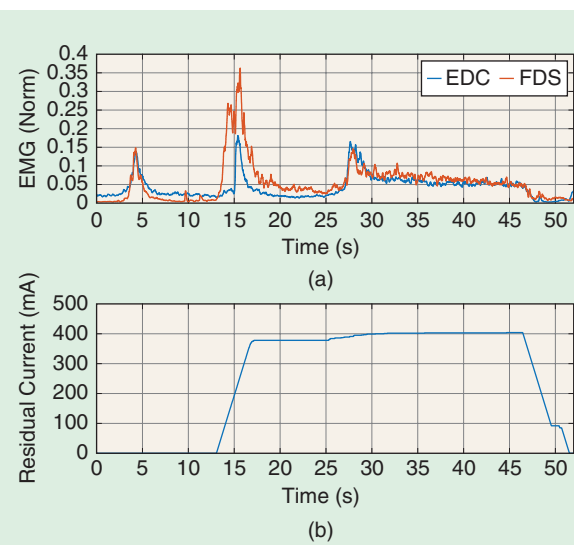


**Figure 6.** The modulation of the EDC and FDS signals and SoftHand grasping force (expressed in terms of residual current) when the user (Subject 1) did not use the CUFF device.

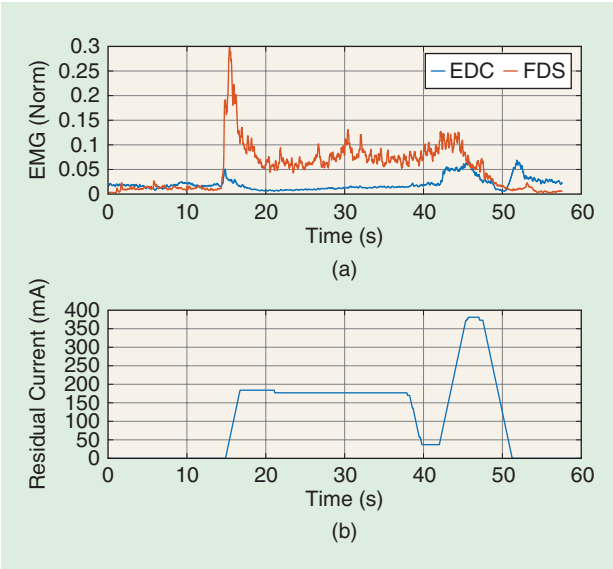


**Figure 7.** The modulation of the EDC and FDS signals and SoftHand grasping force (expressed in terms of residual current) when the user (Subject 1) wore and used the CUFF device.

#### EMG Modulation and Endpoint Stiffness (Changing the P-Gain)

This section illustrates the results of the regulation of the robot endpoint stiffness through control of CMS (contribution of muscular activations) and CDS (through arm geometry). The effect of varying the hand stiffness (by changing the P-gain) and the Cartesian stiffness profiles of KUKA can be assessed on the dynamic performance of the system. We do not expect to see any performance degradation using various P-gains or Cartesian stiffness profiles in terms of trajectory tracking in free space (assuming a reasonable compensation of system uncertainties such as friction). Nevertheless, the

force response of the two systems (hand and robot arm) to the environmental displacements would clearly differ and be determined by the choice of the parameters.

The objective here is to illustrate that certain endpoint impedance profiles and, hence, gains (for hand and KUKA), provide the best performance for certain physical interaction scenarios, as is the case of a drilling task. Thus, since the best performance relies on the choice of gains, we use a human-in-the-loop system to intuitively tune them online. The typical results of the TI control with haptic feedback are illustrated in Figure 8(a) and (b) for two typical subjects, respectively. As illustrated in the plots, the operators could modulate the volume of the Cartesian stiffness profile (a coordinated increase in the matrix components) by applying cocontractions in different phases of the task.

In addition, in robotic arm control, if the control of the endpoint stiffness geometry was necessary, then the proposed method enables the operator to use the effect of configuration to intuitively modulate the stiffness in certain axes of the Cartesian stiffness (e.g., while drilling, the arm is extended on  $x$  direction to achieve a stiffer profile in  $x$  even in small muscular activation levels). Hence, potential misalignments in other directions would not achieve unnecessary high-interaction forces. This explains the change of endpoint stiffness in similar activation levels of the muscles but different arm poses of the operator. The operator's ability to modulate the endpoint stiffness of the KUKA robot (and the consequent restoring forces) according to the needs of the task led to an increase in the success rate.

#### Interaction Forces

Figure 9 illustrates typical acquired interaction forces at the KUKA end effector for the three control modes (LS, HS, and TI) during the drilling task. As observed in the plots, while

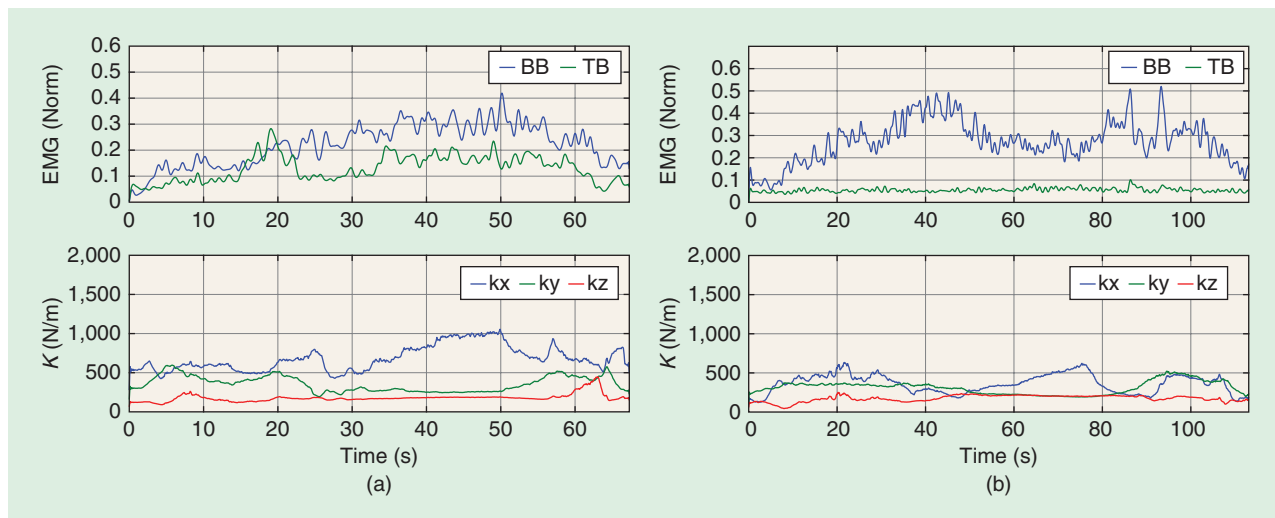


**Figure 8.** A summary of data collected from (a) Subject 1 and (b) Subject 4. The processed (filtered and normalized) EMG signals of the BB and TB muscles are illustrated in the upper plot of each chart during the TI experiment. The resulting human arm endpoint stiffness (that is achieved in the KUKA endpoint using the Cartesian impedance controller of the robot) in the KUKA frame of reference is illustrated in the lower plot of each chart for the TI controller with haptic feedback.  $K$ : torque;  $k_x$ : torque on  $x$ -axis;  $k_y$ : torque on  $y$ -axis;  $k_z$ : torque on  $z$ -axis.

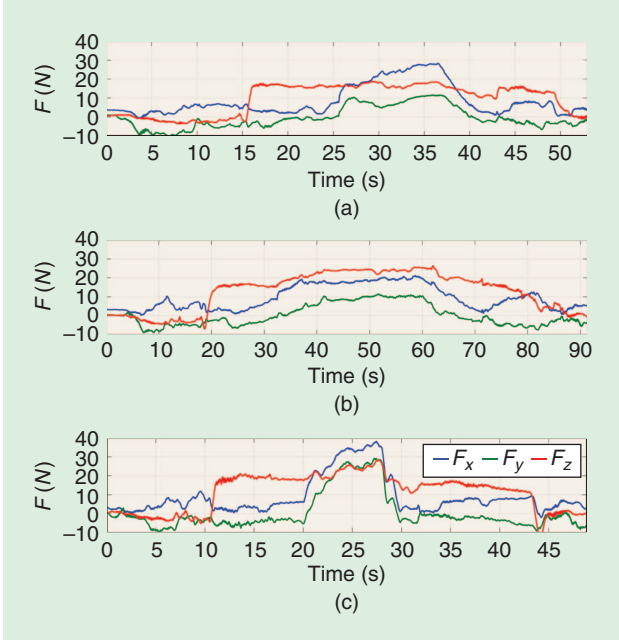


**Figure 9.** The typical acquired interaction forces at the KUKA end effector for the three control modes. All three modes include haptic feedback. (a) TI, (b) LS, and (c) HS.

interaction forces are low in the LS case, the time of the execution is very long compared to the rest of the modes. The HS case, however, achieved an unnecessary high-interaction force in directions other than drilling (e.g., in  $y$  direction), which could cause damage to the tool or the environment. In the TI case, the TI control mode enables the regulation of interaction forces according to the task phase and its requirement, as depicted in Figure 9.

## Conclusions and Future Works

In this article, we discussed the results of human–robot teleoperation in a cooperative object manipulation task, leveraging a wearability paradigm and the generalized simplification approach of human synergies. The task was a drilling task, during which a human user was required to teleoperate a robotic synergy-inspired hand-arm system equipped with the Pisa/IIT SoftHand to grasp and use a driller. A successful task accomplishment required advanced action perception skills, which include both knowledge about the object properties and the execution of motor primitives without increasing the complexity for sensing and control on the robotic side.

To perform this action, we developed a system that integrates in a coherent manner undersensing and wearable haptic feedback devices and augmented teleoperation methods based on TI, which enabled us to safely simply and stably control the position and stiffness of a robotic hand and arm system in the synergy space. Results from a preliminary experimental validation carried out with human participants show that the usage of TI and force feedback seems to increase the success rate and was perceived by participants as a highly valuable and intuitive aid for task accomplishment. The TI mode with haptic feedback enabled subjects to effectively regulate EMG sig-

nals and the interaction forces of the Pisa/IIT SoftHand. Furthermore, the wearability of the sensing glove used to control the position of the robotic hand along the first human grasping synergy was perceived by participants as significantly high. It can be concluded that the presented system seems to increase effectiveness, intuitiveness, and comfort during collaborative tasks performed by a human user and a robot, ensuring stability and the naturalness of HRI for synergy-inspired artificial devices. It is also important to observe that these techniques can be successfully applied and extended to robotic devices with additional degrees of actuation, enabling a simplified and effective human–robot communication.

Future works will focus on further testing this system with a greater number of participants and evaluating other modalities for HPR (e.g., visual based), as well as the effect of other feedback modes (e.g., vibrotactile). The wearability of the overall system will also be pushed further. Envisioned applications include medical robotics, entertainment, and amusement as well as teleoperation in hazardous and remote environments.

## Acknowledgments

We thank Marta Lorenzini and Pietro Balatti for their help in performing the experiments. This work is supported in part by the European Research Council under the advanced grant “SoftHands: A Theory of Soft Synergies for a New Generation of Artificial Hands” (ERC-291166), by the European Union (EU) FP7 project “Wearable Haptics for Humans and Robots” (601165), and from the EU’s Horizon 2020 research and innovation programme under grant agreement No. 688857 (Soft-Pro) and No. 645599 (SOMA). The content of this publication is the sole responsibility of the authors. The European Commission or its services cannot be held responsible for any use that may be made of the information it contains.

## References

- [1] D. A. Lawrence, “Stability and transparency in bilateral teleoperation,” *IEEE Trans. Robot. Autom.*, vol. 9, no. 5, pp. 624–637, 1993.
- [2] B. Hannaford, “A design framework for teleoperators with kinesthetic feedback,” *IEEE Trans. Robot. Autom.*, vol. 5, no. 4, pp. 426–434, 1989.
- [3] J.-H. Ryu, D.-S. Kwon, and B. Hannaford, “Stability guaranteed control: Time domain passivity approach,” *IEEE Trans. Control Syst. Technol.*, vol. 12, no. 6, pp. 860–868, 2004.
- [4] L. Huijun and S. Aiguo, “Virtual-environment modeling and correction for force-reflecting teleoperation with time delay,” *IEEE Trans. Ind. Electron.*, vol. 54, no. 2, pp. 1227–1233, 2007.
- [5] H. Qin, A. Song, Y. Liu, G. Jiang, and B. Zhou, “Design and calibration of a new 6 DoF haptic device,” *Sensors (Basel)*, vol. 15, no. 12, pp. 31,293–31,313, 2015.
- [6] R. E. Schoonmaker and C. G. L. Cao, “Vibrotactile force feedback system for minimally invasive surgical procedures,” in *Proc. 2006 IEEE Int. Conf. Systems, Man and Cybernetics*, vol. 3, Oct. 2006, pp. 2464–2469.
- [7] D. Prattichizzo, C. Pacchierotti, and G. Rosati, “Cutaneous force feedback as a sensory subtraction technique in haptics,” *IEEE Trans. Haptics*, vol. 5, no. 4, pp. 289–300, 2012.

- [8] X. Xu, A. Song, D. Ni, H. Li, P. Xiong, and C. Zhu, "Visual-haptic aid teleoperation based on 3-D environment modeling and updating," *IEEE Trans. Ind. Electron.*, vol. 63, no. 10, pp. 6419–6428, 2016.
- [9] A. Ajoudani, *Transferring Human Impedance Regulation Skills to Robots*. Switzerland: Springer International Publishing, 2016.
- [10] C. Della Santina, M. Bianchi, G. Grioli, M. G. Catalano, M. Garabini, and A. Bicchi, "Controlling soft robots: balancing feedback and feedforward elements," *IEEE Robot. Autom. Mag.*, vol. 24, no. 3, pp. 75–83, 2017.
- [11] M. Bianchi, "A fabric-based approach for wearable haptics," *Electronics*, vol. 5, no. 3, pp. 44, 2016.
- [12] C. Pacchierotti, F. Chinello, M. Malvezzi, L. Meli, and D. Prattichizzo, "Two finger grasping simulation with cutaneous and kinesthetic force feedback," in *Haptics: Perception, Devices, Mobility and Communication*. Berlin, Germany: Springer-Verlag, 2012, pp. 373–382.
- [13] M. Santello, M. Flanders, and J. F. Soechting, "Postural hand synergies for tool use," *J. Neuroscience*, vol. 18, no. 23, pp. 10,105–10,115, 1998.
- [14] M. Santello, M. Bianchi, M. Gabiccini, E. Ricciardi, G. Salvietti, D. Prattichizzo, M. Ernst, A. Moscatelli, H. Jorntell, A. Kappers, K. Kyriakopoulos, A. Albu-Schaeffer, C. Castellini, and A. Bicchi. (2016, July). Hand synergies: Integration of robotics and neuroscience for understanding the control of biological and artificial hands. *Physics Life Rev.* [Online]. 17, pp. 1–23. Available: <http://www.sciencedirect.com/science/article/pii/S1571064516000269>
- [15] M. G. Catalano, G. Grioli, E. Farnioli, A. Serio, C. Piazza, and A. Bicchi, "Adaptive synergies for the design and control of the Pisa/IIT softhand," *Int. J. Robotics Res.*, vol. 33, no. 5, pp. 768–782, 2014.
- [16] S. Casini, M. Morvidoni, M. Bianchi, M. Catalano, G. Grioli, and A. Bicchi, "Design and realization of the CUFF—Clenching upper-limb force feedback wearable device for distributed mechano-tactile stimulation of normal and tangential skin forces," in *Proc. 2015 IEEE/RSJ Int. Conf. Intelligent Robots and Systems (IROS)*, Sept. 2015, pp. 1186–1193.
- [17] A. Ajoudani, S. B. Godfrey, M. Bianchi, M. G. Catalano, G. Grioli, N. Tsagarakis, and A. Bicchi, "Exploring teleimpedance and tactile feedback for intuitive control of the Pisa/IIT softhand," *IEEE Trans. Haptics*, vol. 7, no. 2, pp. 203–215, 2014.
- [18] S. Ciotti, E. Battaglia, N. Carbonaro, A. Bicchi, A. Tognetti, and M. Bianchi, "A synergy-based optimally designed sensing glove for functional grasp recognition," *Sensors (Basel)*, vol. 16, no. 6, pp. E811, 2016.
- [19] A. Ajoudani, C. Fang, N. G. Tsagarakis, and A. Bicchi, "A reduced-complexity description of arm endpoint stiffness with applications to teleimpedance control," in *Proc. 2015 IEEE/RSJ Int. Conf. Intelligent Robots and Systems (IROS)*, Hamburg, Germany, Sept./Oct. 2015, pp. 1017–1023.
- [20] T. E. Milner, "Contribution of geometry and joint stiffness to mechanical stability of the human IJM," *Exp. Brain Res.*, vol. 143, pp. 515–519, 2002.
- [21] S. L. Delp, F. C. Anderson, A. S. Arnold, P. Loan, A. Habib, C. T. John, E. Guedelman, and D. G. Thelen, "OpenSim: Open-source software to create and analyze dynamic simulations of movement," *IEEE Trans. Biomed. Eng.*, vol. 54, no. 11, pp. 1940–1950, 2007.
- [22] E. Van Zuylen, C. Gielen, and J. D. Van Der Gon, "Coordination and inhomogeneous activation of human arm muscles during isometric torques," *J. Neurophysiol.*, vol. 60, no. 5, pp. 1523–1548, 1988.
- [23] R. Osu and H. Gomi, "Multijoint muscle regulation mechanisms examined by measured human arm stiffness and emg signals," *J. Neurophysiol.*, vol. 81, no. 4, pp. 1458–1468, 1999.
- [24] M. T. Turvey, "Action and perception at the level of synergies," *Hum. Movement Sci.*, vol. 26, no. 4, pp. 657–697, 2007.
- [25] P. Pigeon, L. Yahia, and A. G. Feldman, "Moment arms and lengths of human upper limb muscles as functions of joint angles," *J. Biomech.*, vol. 29, no. 10, pp. 1365–1370, 1996.
- [26] M. Bianchi, R. Haschke, G. Büscher, S. Ciotti, N. Carbonaro, and A. Tognetti, "A multi-modal sensing glove for human manual-interaction studies," *Electron.*, vol. 5, no. 3, p. 42, 2016.
- [27] A. Tognetti, F. Lorussi, G. Dalle Mura, N. Carbonaro, M. Pacelli, R. Paradiso, and D. De Rossi, "New generation of wearable goniometers for motion capture systems," *J. Neuroengineering Rehabil.*, vol. 11, no. 1, p. 1, 2014.
- [28] M. Bianchi, P. Salaris, and A. Bicchi, "Synergy-based hand pose sensing: Optimal glove design," *Int. J. Robotics Res.*, vol. 32, no. 4, pp. 407–424, 2013.
- [29] M. Bianchi, P. Salaris, and A. Bicchi, "Synergy-based hand pose sensing: Reconstruction enhancement," *Int. J. Robotics Res.*, vol. 32, no. 4, pp. 396–406, 2013.
- [30] A. Bicchi, M. Gabiccini, and M. Santello, "Modelling natural and artificial hands with synergies," *Philos. T. Roy. Soc. B*, vol. 366, no. 1581, pp. 3153–3161, 2011.
- [31] C. Della Santina, G. Grioli, M. Catalano, A. Brando, and A. Bicchi, "Dexterity augmentation on a synergistic hand: The Pisa/IIT soft-hand+," in *Proc. 2015 IEEE-RAS 15th Int. Conf. Humanoid Robots (Humanoids)*, Seoul, Korea, Nov. 2015, pp. 497–503.
- [32] S. Fani, M. Bianchi, S. Jain, J. S. P. Neto, S. Boege, G. Grioli, A. Bicchi, and M. Santello, "Assessment of myoelectric controller performance and kinematic behavior of a novel soft synergy-inspired robotic hand for prosthetic applications," *Front. Neurorobot.*, vol. 10, 2016.

**Simone Fani**, Enrico Piaggio Research Center, University of Pisa, Italy, and Department of Advanced Robotics, Istituto Italiano di Tecnologia, Genova, Italy. E-mail: s.fani@centropiaggio.unipi.it.

**Simone Ciotti**, Enrico Piaggio Research Center, University of Pisa, Italy, and Department of Advanced Robotics, Istituto Italiano di Tecnologia, Genova, Italy. E-mail: simone.ciotti@centropiaggio.unipi.it.

**Manuel G. Catalano**, Department of Advanced Robotics, Istituto Italiano di Tecnologia, Genova, Italy. E-mail: manuel.catalano@iit.it.

**Giorgio Grioli**, Department of Advanced Robotics, Istituto Italiano di Tecnologia, Genova, Italy. E-mail: giorgio.grioli@iit.it.

**Alessandro Tognetti**, Enrico Piaggio Research Center, University of Pisa, Italy. E-mail: alessandro.tognetti@centropiaggio.unipi.it.

**Gaetano Valenza**, Enrico Piaggio Research Center and Department of Information Engineering, University of Pisa, Italy. E-mail: gaetano.valenza@ing.unipi.it.

**Arash Ajoudani**, Department of Advanced Robotics, Istituto Italiano di Tecnologia, Genova, Italy. E-mail: arash.ajoudani@iit.it.

**Matteo Bianchi**, Enrico Piaggio Research Center and Department of Information Engineering, University of Pisa, Italy. E-mail: matteo.bianchi@centropiaggio.unipi.it.